

Chapter 9

Modeling Atmospheric HONO Concentrations on the Regional Scale

Bernhard Vogel and Heike Vogel

Abstract Mechanisms to simulate the formation of nitrous acid (HONO), an important OH radical source in the atmosphere, have been incorporated into numerical models. The results from the model simulations of HONO formation are compared with field measurements of HONO and conclusions are drawn regarding HONO formation mechanisms in the atmosphere and their representation in models.

Keywords Model • Regional scale • Nitrous acid

9.1 Introduction

Nitrous acid (HONO) is an important nitrogen compound of the atmosphere as it is involved in the OH budget. However, the formation of HONO is currently still not understood. Recent investigations have shown that numerical models that include only homogeneous gas phase reactions of HONO are not able to simulate the observed HONO concentrations. Even when direct emissions and heterogeneous reactions at surfaces are taken into account the concentrations of HONO are underestimated and some of the observed features are not represented by atmospheric models. Investigations of Vogel et al. [13] and Sarwar et al. [11] have shown that including a hypothetical photolytic source of HONO improves the model results considerably when compared with measurements. In this study we will present 1-D simulations of Vogel et al. [13] and recently performed 3-D simulations with the new model system COSMO-ART.

B. Vogel (✉) • H. Vogel

Institute for Meteorology and Climate Research, Karlsruhe Institute of Technology,
Karlsruhe, Germany

e-mail: bernhard.vogel@kit.edu

9.2 The Model System

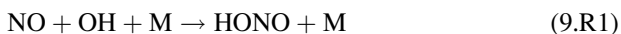
The model system COSMO-ART, where ART stands for Aerosols and Reactive Trace gases [14] is an enhanced model system to simulate the spatial and temporal distributions of reactive gaseous and particulate matter. It is used to quantify the feedback processes between aerosols and the state of the atmosphere on the continental to the regional scale with two-way interactions between different atmospheric processes. The meteorological driver is the operational weather forecast model COSMO [2] of the German Weather Service (DWD). In addition to MADEsoot the treatment of mineral dust, sea salt, and pollen bacteria was added to the aerosol module.

The advantage of COSMO-ART with respect to other models is that identical numerical schemes and parameterizations are used for identical physical processes as advection and turbulent diffusion. This avoids truncation errors and model inconsistencies. COSMO is verified operationally by DWD, the model system can be embedded by one way nesting into individual global scale models as the GME model of DWD or the IFS model of ECMWF. All components of the model system are coupled on line with time steps on the order of tenth of seconds. Nesting of COSMO-ART within COSMO-ART is possible. Typical horizontal grid sizes vary between 2.8 and 28 km.

The model system treats secondary aerosols as well as directly emitted components like soot, mineral dust, sea salt, volcanic ash and biological material. Secondary aerosol particles are formed from the gas phase. Therefore, a complete gas phase mechanism (RADMKA) is included in COSMO-ART. Modules for the emissions of biogenic precursors of aerosols, mineral dust, sea salt, biomass burning aerosol and pollen grains are included. For the treatment of secondary organic aerosol (SOA) chemistry the volatility basis set (VBS) was included. Wet scavenging and in-cloud chemistry are taken into account [7]. Processes as emissions, coagulation, condensation (including the explicit treatment of the soot aging; [9, 10]), deposition, washout and sedimentation are taken into account. In order to simulate the interaction of the aerosol particles with radiation and the feedback of this process with the atmospheric variables the optical properties of the simulated particles are parameterized based on detailed Mie-calculations [4]. New methods to calculate efficiently the photolysis frequencies and the radiative fluxes, based on the actual aerosol load and on the GRAALS radiation scheme, respectively, were developed and are implemented in COSMO-ART. To simulate the impact of the various aerosol particles on the cloud microphysics and precipitation COSMO-ART was coupled with the two-moment cloud microphysics scheme of Seifert and Beheng [12] by using comprehensive parameterisations for aerosol activation and ice nucleation [3].

9.3 Treatment of HONO

As regards HONO, the following gas phase reactions are taken into account:



This reaction is the most important gas phase source of HONO. For the rate constant of 9.R1, the recent IUPAC recommendation of $9.7 \cdot 10^{-12} \text{ cm}^{-6} \text{ s}^{-1}$ [1] is used. During daytime, HONO is photolyzed:



Since the highest HONO concentrations are reached during the night, it is obvious that there must be additional sources of HONO. Following the results of a tunnel study of Kurtenbach et al. [8], a direct HONO source is included in the lowest model layer proportional to the emissions of NO ($E_{\text{HONO}} = 0.008 \cdot E_{\text{NO}}$).

In addition, the following heterogeneous reaction [5] is included:



This heterogeneous reaction which was found to be of first order in $[\text{NO}_2]$ in laboratory studies is implemented with the following rate constant:

$$k_{\text{het}} = 3 \cdot 10^{-3} \text{ m min}^{-1} \cdot S/V \quad (9.1)$$

S/V is the surface to volume ratio. This rate constant is based on a tunnel study [8] where an effective uptake coefficient for NO_2 of $\gamma_{\text{NO}_2} = 10^{-6}$ was found on a tunnel surface. To take into account the heterogeneous production of HONO at aerosol surfaces, S/V in Eq. (9.1) is replaced by the simulated aerosol surface density. To consider the heterogeneous reactions directly on the ground, a source of HONO is introduced in the lowest model layer and it is assumed that the surface to volume ratio of this model layer is 0.1 m^{-1} . This is equivalent to an effective surface of 1.7 m^2 per geometric surface in this layer. Furthermore, we implemented a hypothetical photolytic source of HONO:



In the model this reaction is realized as an additional source of HONO at the surface:

$$E_{\text{HONO}} = A \cdot J_{\text{NO}_2} \quad (9.2)$$

E_{HONO} is the rate of HONO formation by the photolytic source, A is a tuning parameter and J_{NO_2} is the photolysis rate coefficient of NO_2 . Actually, we do not know by which species X should be replaced in (9.R4). In our case we used the photolysis rate constant of NO_2 . However, that does not mean that we think that NO_2 is the missing species. A is the product of the concentration of the unknown species X and an additional factor. In our study we assumed that A is constant with time and used that parameter for the tuning of our model.

9.4 Model Simulations

We used a hierarchy of model versions for a systematic investigation of the improved description of the processes involved in HONO formation and their influence on the photo-oxidant production. We carried out one-dimensional

simulations with KAMM/DRAIS including MADEsoot [13] to quantify the effects of different processes in a more systematic way. Then we performed three-dimensional simulations to investigate the effects of the individual processes important for HONO in the real atmosphere when transport processes and the spatial distribution of the sources and sinks of the gaseous and particulate trace constituents interact with the chemical processes. As HONO acts as an OH source it alters not only the gas phase concentrations but also the chemical composition of the aerosol particles.

9.5 1-D Simulations

Assuming horizontal homogeneous conditions we performed sensitivity runs for October 18, 2001. For the reference case (R) direct emissions of HONO and heterogeneous reactions at the aerosol surface and at the ground were taken into account together with the gas-phase reactions. For the cases E and S the direct emissions of HONO (E) and the heterogeneous reactions at the surface (S) were switched off, respectively. Figure 9.1 shows simulated daily cycles of HONO at 17 m above surface for the cases R, E, and S together with the observations taken at a tower at KIT. In case R the simulated nighttime concentrations are in reasonable agreement with the observations. After 9:00 CET the observations are underestimated. During daytime the simulated HONO concentrations are 30–50% lower than the observed ones. When the direct emissions of HONO are switched off (E), the HONO concentrations are reduced by 50% at maximum between 06:00 CET and 09:00 CET. Between 21:00 CET and 28:00 CET this difference reduces to 40% (Fig. 9.2, *left*). When the heterogeneous reactions are switched off (S) the early morning concentrations of HONO are reduced by 25% between 06:00 and 09:00 CET, and by 30% between 21:00 CET and 28:00 CET.

In all cases the simulated HONO concentrations during daytime do not differ too much but are 30–50% lower than the observations. This shows that there must be an additional strong HONO source during the day. Therefore an artificial photolytic HONO source (P) was introduced. Figure 9.2 (*right*) shows that we received a much better agreement between measured and simulated concentrations of HONO. Especially the decrease of HONO between 9:00 CET and 12:00 CET was simulated very well and the HONO concentrations around noon are comparable to the observed ones. The conclusions from this 1-D simulations are: During daytime the simulated HONO concentrations for the individual cases are much lower than the observed ones. The additional photolytic source of HONO gives much better results. Nighttime HONO concentration close to the surface is simulated quite well. HONO production on aerosols plays no role. Direct emissions of HONO and heterogeneous production of HONO at the ground contribute by the same amount to the sources of HONO during the night. Above 100 m larger differences for the HONO concentrations are found. Possible reasons are transport effects.

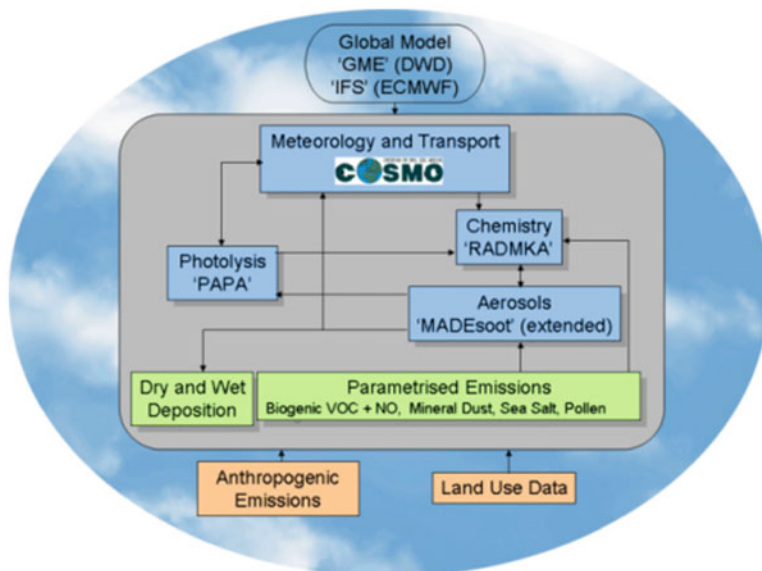


Fig. 9.1 The model system COSMO-ART

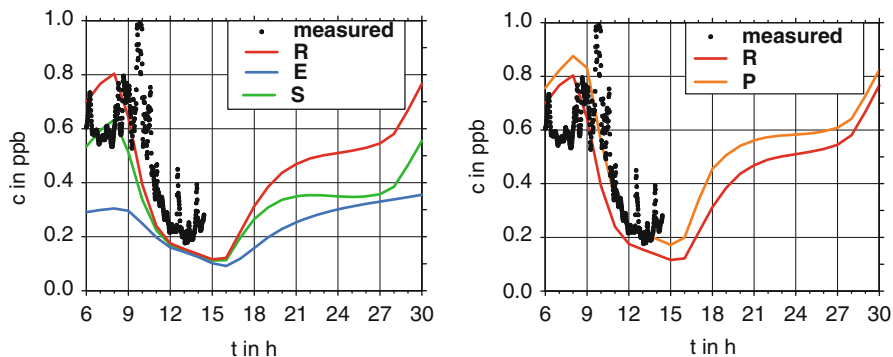


Fig. 9.2 Observed and simulated daily cycles of the HONO concentration at October 18, 2001. *R* reference case, *E* with HONO emissions, *S* the heterogeneous reaction at the surface, *P* with photolytic source. Hour 6 is identical to 6:00 CET at October 18, 2001

9.6 3-D Simulations

Simulations with the CMAQ modeling systems were carried out for the summer 2001 and compared with observations [11]. Taken into account only gas phase reactions gives to low HONO concentrations and show also a different diurnal cycle in comparison to the measurements. Adding the heterogeneous reaction of HONO at ground surfaces as well as at aerosol surfaces with a rate constant of

$3 \times 10^{-3} \text{ S/V m}^{-1}$ (S/V is the ratio of surface area to volume of air) leads to much better agreement for the night. A major uncertainty is the estimation of the surface areas of the structures in urban environments. Zhou et al. [16] proposed a production of HONO and NO_2 during the day due to photolysis of adsorbed HNO_3 . Implementing this source leads to a remarkable increase of the HONO concentration during the day. This implies the need of further investigation of this reaction.

Using COSMO-ART simulations were carried out for an ozone episode in June 2006. We performed five sensitivity runs. In the first run (Gas phase, Standard) gas phase reactions were taken into account only. The second run (E & het R) accounts for direct emissions of HONO and heterogeneous reactions (9.R3). With respect to the photolytic reaction we introduced two separate parameterizations. In the first case the photolytic source was switched on (Eq. 9.1 with $A = 2.5 \cdot 10^{-4}$) when the actual HNO_3 concentration close to the surface was above 1 ppb over land (E & het R & P (const)). In the second one the photolytic source was switched on when the actual HNO_3 concentration close to the surface was above 1 ppb and the following equation was applied (E & het R & P (const)) to modulate the photolytic source according to the HNO_3 concentration in ppb.

$$E_{\text{HONO}} = A \cdot J_{\text{NO}_2} \cdot [\text{HNO}_3]/5 \quad (9.3)$$

Figure 9.3 shows as an example the horizontal distributions of NO_x , HONO (13 June, 6 UTC), HNO_3 , and ozone (June 13, 2006, 13 UTC). Concerning NO_x and HONO a good correlation with the emission distribution can be recognized whereas for ozone and HNO_3 the highest concentrations can be also found in the western part of Germany and Northern Italy but the pattern are more homogeneous. Figure 9.4 gives the temporal development of the HONO concentrations at the grid point of the tower of KIT for the time interval June 10,–13, 2006. Again different sensitivity runs were performed. Even though horizontal transport processes were now taken into account the calculated HONO concentration is rather low if only gas phase reactions are considered. The implementation of a photolytic source over land areas leads to an increase of the HONO concentration. The blue curve in Fig. 9.4 shows the result for a constant source whereas the red line represents the case when the source is a function of the HNO_3 concentration. Remarkable differences between these two runs occur except of the 2nd day during the night. A similar behavior can be seen in Fig. 9.5, which shows the according ratio of HONO/NO_x .

Also in discussion is the question if the HONO concentration shows a distinct profile with height or not. Häslér et al. [6] analyzed Zeppelin measurements up to 1,000 m height and found almost no gradient of the mean HONO concentration. Zhang et al. [15] showed measured profile at different sites and found no clear behavior. Figure 9.5 gives the simulated concentrations profiles of HONO at different point of time. One can recognize a sharp gradient close to the surface and above a well-mixed layer with almost no gradient with height. The same feature can be found for the ratio HONO/NO_x .

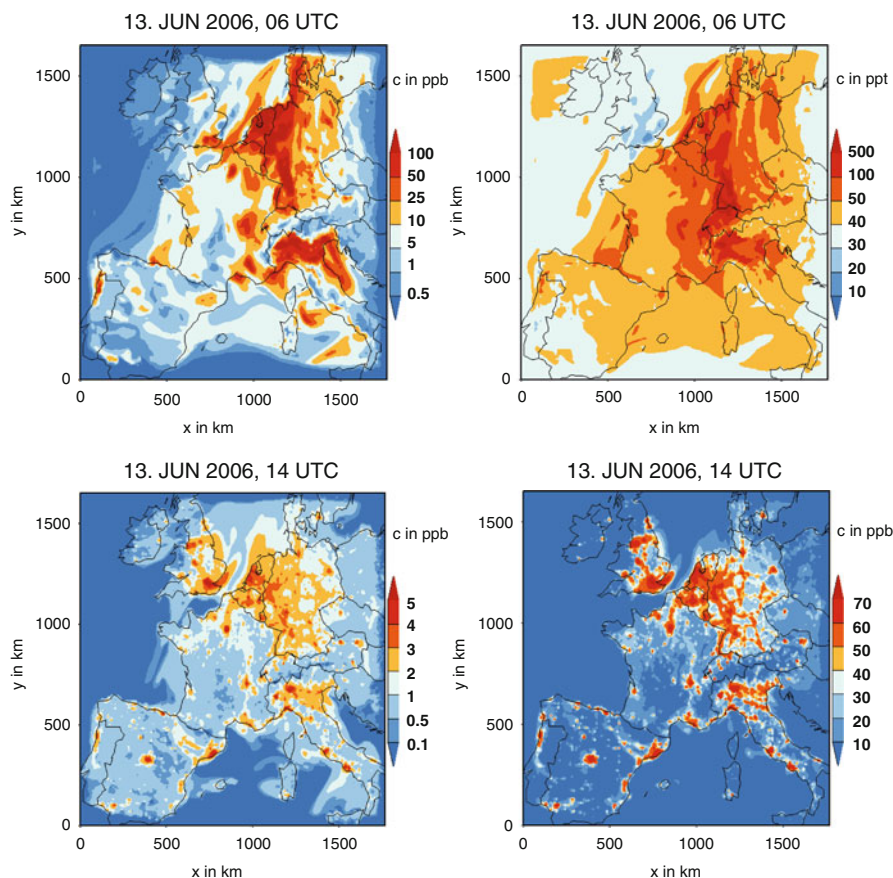


Fig. 9.3 Simulated horizontal distributions of NO_x , HONO, HNO_3 , and O_3 at ~ 20 m above ground ((E & het R & P (const))

HONO is an important species in case of ozone formation especially in the early morning hours. Therefore it raises the question which changes can be found in the OH and also in the ozone concentrations when the additionally sources for HONO are included in the model run. Figure 9.7 shows the temporal development of OH and ozone for the sensitivity runs. The implementation of the HONO emissions and the heterogeneous reaction at the surface has no impact on the OH concentration. If the photolytic source is added an increase of the OH concentration of up to 30% during the day can be seen. In contrast to this finding no clear effect on the ozone concentration can be found. The higher HONO concentrations lead only to very small increase of the ozone concentration. Similar results were found by Sarwar et al. [11].

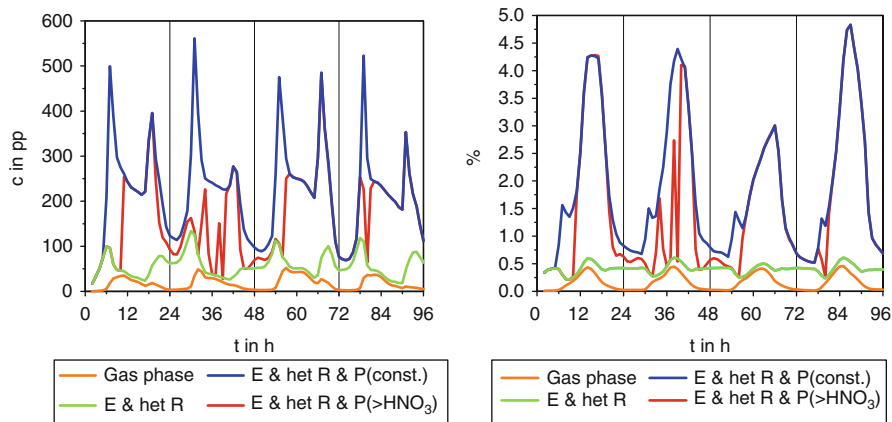


Fig. 9.4 Simulated daily cycles of the HONO concentration (*left*) and HONO/NO_x (*right*) at grid point Karlsruhe (June 10–13, 2006)

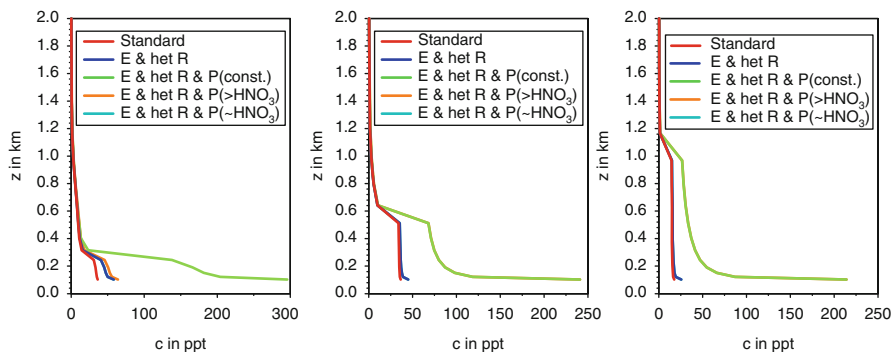


Fig. 9.5 Simulated vertical profiles of the HONO concentration at 8.00, 11:00 and 14:00 CET

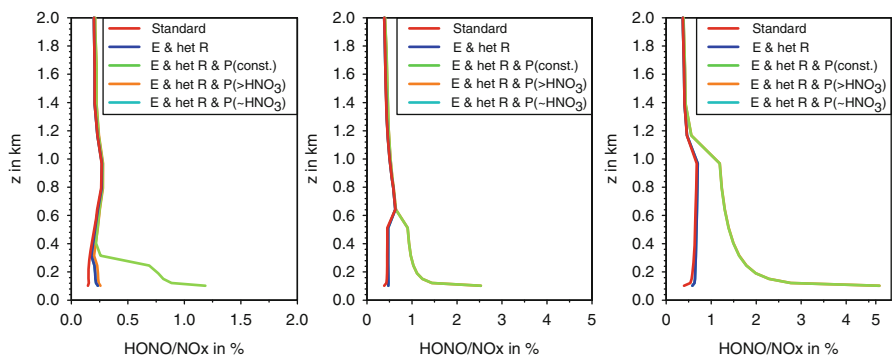


Fig. 9.6 Simulated vertical profiles of the HONO/NO_x at 8.00, 11:00 and 14:00 CET

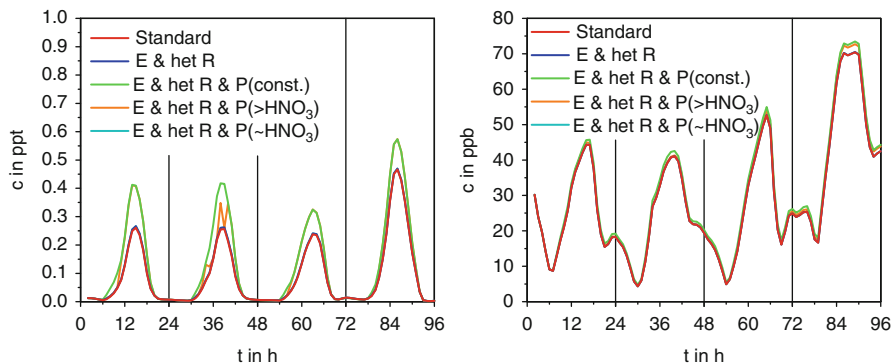


Fig. 9.7 Simulated daily cycles of OH (*left*) and O₃ (*right*) concentration at grid point Karlsruhe (June 10–13, 2006)

9.7 Conclusions

From the 1-D simulations we could see that during daytime the simulated HONO concentrations for the individual cases were much lower than the observed ones. Adding an additional photolytic source of HONO gives much better results. For the nighttime the HONO concentration close to the surface was simulated quite well. Direct emissions of HONO and heterogeneous production of HONO at the ground contribute by the same amount to the sources of HONO during the night. Above 100 m larger differences for the HONO concentrations are found.

The 3-D simulations showed also that introducing a daytime source proportional to radiation or surface temperature leads to HONO concentrations comparable to observed ones close to the surface. It is still not clear what kind of source this is. With respect to the vertical profiles the picture is still not clear. If HONO would be constant with height throughout the convective boundary layer a very strong source is missing. Concerning ozone our results show that even if we simulate HONO concentrations close to the observations the impact on ozone and also other species is smaller than one might expect.

References

1. Atkinson R, Baulch DL, Cox RA, Crowley JN, Hampson RF, Hynes RG, Jenkin ME, Rossi MJ, Troe J (2004) Evaluated kinetic and photochemical data for atmospheric chemistry: volume I gas phase reactions of Ox, HOx, NOx, and SOx, species, *Atmos Chem Phys* 4:1461–1738
2. Baldauf M, Seifert A, Foerstner J, Majewski D, Raschendorfer M, Reinhardt T (2011) Operational convective-scale numerical weather prediction with the COSMO model: description and sensitivities. *Mon Weather Rev* 139:3887–3905. doi:[10.1175/MWR-D-10-05013.1](https://doi.org/10.1175/MWR-D-10-05013.1), e-View, 2011. 31941, 31942

3. Bangert M, Kottmeier C, Vogel B, Vogel H (2011) Regional scale effects of the aerosol cloud interaction simulated with an online coupled comprehensive chemistry model. *Atmos Chem Phys* 11:4411–4423. doi:[10.5194/acp-11-4411-2011](https://doi.org/10.5194/acp-11-4411-2011)
4. Geleyn J-F, Ritter B (1992) A comprehensive radiation scheme for numerical weather prediction models with potential applications in climate simulations. *Mon Weather Rev* 120:303–325
5. Harris GW, Carter WPL, Winer AM, Pitts JN Jr, Platt U, Perner D (1982) Observations of nitrous acid in the Los Angeles atmosphere and the implications for the ozone-precursor relationships. *Environ Sci Technol* 16:414–419
6. Häselner R, Brauers T, Holland F, Wahner A (2009) Development and application of a new mobile LOPAP instrument for the measurement of HONO altitude profiles in the planetary boundary layer. *Atmos Meas Tech Discuss* 2:2027–2054. doi:[10.5194/amtd-2-2027-2009](https://doi.org/10.5194/amtd-2-2027-2009)
7. Knote C, Brunner D, Vogel H, Allan J, Asmi A, Äijälä M, Carbone S, van der Gon HD, Jimenez JL, Kiendler-Scharr A, Mohr C, Poulain L, Prévôt ASH, Swietlicki E, Vogel B (2011) Towards an online-coupled chemistry-climate model: evaluation of trace gases and aerosols in COSMO-ART. *Geosci Model Dev* 4:1077–1102. doi:[10.5194/gmd-4-1077-2011](https://doi.org/10.5194/gmd-4-1077-2011)
8. Kurtenbach R, Becker K, Gomes J, Kleffmann J, Lorzer J, Spittler M, Wiesen P, Ackermann R, Geyer A, Platt U (2001) Investigations of emissions and heterogeneous formation of HONO in a road traffic tunnel. *Atmos Environ* 35:3385–3394
9. Riemer N, Vogel H, Vogel B, Schell B, Ackermann I, Kessler C, Hass H (2003) The impact of the heterogeneous hydrolysis of N₂O₅ on tropospheric chemistry and nitrate aerosol formation. *J Geophys Res* 108:4144. doi:[10.1029/2002JD002436](https://doi.org/10.1029/2002JD002436)
10. Riemer N, Vogel H, Vogel B (2004) Soot aging time scales in polluted regions during day and night. *Atmos Chem Phys* 4:1885–1893, SRef-ID: 1680-7324/acp/2004-4-1885
11. Sarwar G, Roselle S, Mathur R, Appel W, Dennis RL, Vogel B (2008) A comparison of CMAQ HONO predictions with observations from the northeast oxidant and particle study. *Atmos Environ* 42:5760–5770. doi:[10.1016/j.atmosenv.2007.12.065](https://doi.org/10.1016/j.atmosenv.2007.12.065)
12. Seifert A, Beheng KD (2006) A two-moment cloud microphysics parameterization for mixed-phase clouds. Part 1: model description. *Meteorol Atmos Phys* 92:45–66. doi:[10.1007/s00703-005-0112-4](https://doi.org/10.1007/s00703-005-0112-4). 31942, 31943, 31944, 31946, 31947
13. Vogel B, Vogel H, Kleffmann J, Kurtenbach R (2003) Measured and simulated vertical profiles of nitrous acid, part II – model simulations and indications for a photolytic source. *Atmos Environ* 37:2957–2966
14. Vogel B, Vogel H, Bäumer D, Bangert M, Lundgren K, Rinke R, Stanelle T (2009) The comprehensive model system COSMO-ART – radiative impact of aerosol on the state of the atmosphere on the regional scale. *Atmos Chem Phys* 9:8661–8680
15. Zhang N, Zhou X, Shepson PB, Gao H, Alaghmand M, Stirm B (2009) Aircraft measurements of HONO vertical profiles over a forested region. *Geophys Res Lett* 36:L15820. doi:[10.1029/2009GL038999](https://doi.org/10.1029/2009GL038999)
16. Zhou X, Gao H, He Y, Huang G, Bertman S, Civerolo K, Schwab J (2003) Nitric acid photolysis on surfaces in low-NO_x environments: significant atmospheric implications. *Geophys Res Lett* 30(23):2217. doi:[10.1029/2003GL018620](https://doi.org/10.1029/2003GL018620)